

An Investigation of Diffusion Welding of Pure and Alloyed Aluminum to Type 316 Stainless Steel

The tensile strengths of stainless steel/aluminum or aluminum alloy welds are functions of time and temperature of aging, and weld mechanical property changes are correlated with intermetallic phases forming between stainless steel and aluminum

BY P. D. CALDERON, D. R. WALMSLEY, AND Z. A. MUNIR

ABSTRACT. Using silver as an intermediate layer, samples of Type 316 stainless steel specimens were diffusion welded to two aluminum alloys (1100 and 6061) and to 99.99% pure aluminum, utilizing the hot hollow cathode faying surface coating technique. The three types of welds formed were aged at temperatures ranging from 423 to 513 K* (302 to 464°F), and their tensile strengths were determined as functions of time and temperature of aging.

Little or no change in weld strength was observed with specimens aged at 423 K (302°F). In contrast, specimens aged at 473 and 513 K (392 and 464°F) experienced a significant decrease in their tensile strength and by as much as 60%

for the 1100 alloy. Changes in the mechanical properties of the welds were correlated with the formation and growth of intermetallic phases between silver and aluminum. Microscopic and electron microprobe analyses of aged welds showed the formation of Ag_2Al with smaller amounts of Ag_3Al .

Variations in the weld strength of the three joint types investigated are discussed in light of differences in the morphologies of the silver-aluminum interfaces and the existence of voids at the weld interface.

Introduction

The use of diffusion welding as a joining method has been successfully demonstrated in a variety of cases involving similar and dissimilar metals (Refs. 1-5). As is explicitly indicated by the designation of this joining method, diffusional processes are essential in establishing a metallic bond between faying surfaces. For these transport processes to be operative, surfaces which are to be joined must be brought in intimate contact. Also, for them to be effective, atomic mobilities must be sufficiently high to cause mass transport across and along

the interface. In practical terms these requirements can be satisfied by the application of pressure to bring about better surface-surface contacts and by increasing the temperature to enhance atomic mobilities.

Diffusion welded joints have been made with the aid of an intermediate layer. Such layers are used in the form of foils (Ref. 6) or are deposited onto the surfaces to be joined by electrolytic (Refs. 4, 7) or vapor phase techniques (Ref. 5). The effect of this layer on the properties of the resulting joint depends upon interdiffusion (Ref. 8) and the formation of brittle intermetallic phases (Refs. 9, 10). When aluminum alloys were joined to stainless steel with silver as an intermediate layer, the formation of two intermetallic compounds was observed (Refs. 9, 10). The predominant compound, zeta phase, Ag_2Al , is formed near the aluminum-silver interface and smaller amounts of the mu phase, Ag_3Al , are formed at the silver-rich boundary of Ag_2Al (Ref. 10).

In the cited work of Doyle *et al.* (Ref. 9), it was observed that the strength of the weld between 1100 aluminum and Type 316 stainless steel decreased with increasing thickness of the total interme-

*273 K = 0°C (or 0 K = -273.1°C).

P. D. CALDERON is with the Medical Systems Group, General Electric Co., Fremont, California; D. R. WALMSLEY is with the Lawrence Livermore National Laboratory, Livermore, California; and Z. A. MUNIR is Professor and Associate Dean, Graduate Studies, Division of Materials Science and Engineering, College of Engineering, University of California, Davis, California.

talic layer, with an abrupt decrease occurring at a total thickness of 10 μm . In the work of Naimon *et al.* (Ref. 10), however, the joint tensile strength decreased linearly with increasing intermetallic thickness to the maximum thickness investigated of approximately 21 μm^* .

More revealing, however, is the dependence of the impact strength on intermetallic thickness. Because of the brittle nature of the newly formed phase, its effect on impact strength is drastic. Naimon *et al.* (Ref. 10) showed that an intermetallic layer of more than approximately 4 μm causes the joint to become markedly brittle. At a thickness of about 6 μm , the impact strength is approximately 5 joules for joints between 1100 aluminum alloy and Type 316 stainless steel bars with 0.76 cm (0.3 in.) diameters.

Since the formation and growth of the intermetallic phase are diffusion controlled, the parameters of temperature and time play a dominant role. Naimon *et al.* (Ref. 10) found that during welding carried out at 117 MPa (17 ksi) and 477 K (399°F) for 10 min, the intermetallic Ag₂Al formed and grew to a thickness of approximately 0.5 μm . Subsequent isothermal heating of the joints showed a linear dependence of the thickness of the intermetallic layer with the square-root of time.

In pure metals, the formation of intermetallic compounds, as dictated by phase equilibria, is dependent upon temperature and time only. In dealing with interdiffusion between commercial alloys, however, other factors may play a significant role. In the limit, the nature of the intermetallic compounds may be altered by the presence of alloying elements through the direct chemical involvement of these elements in the formation of a new phase. More likely, however, is the effect of these alloying elements on the mechanism of diffusion and hence kinetics of formation and growth of the intermetallic phases. To examine this phenomenon, an experimental investigation was conducted on samples of Type 316 stainless steel welded to pure aluminum, and to 6061 and 1100 aluminum alloys.

Experimental Materials and Methods

The materials used in this investigation are listed in Table 1 along with their compositions and heat treatment histories. A limited number of determinations of the initial mechanical properties of the 6061 and 1100 alloys were made. These included Brinell hardness measurements for the two alloys and the ultimate and

yield strengths for the 1100 alloy.

With a 500 kg (1102 lb) load and a 10 mm (0.39 in.) ball, the Brinell hardness for the 1100 alloy was determined as 33, a value corresponding to condition H14 with a reported literature (Ref. 11) value of 32. The hardness of the 6061 alloy was measured on as-welded specimens with a result of 93 on the same Brinell scale. This value is slightly lower than the reported value (Ref. 11) of 95 for condition T6. It is believed that the relatively short welding time of 10 min at 477 K (399°F) is not sufficient to cause significant changes in the hardness of the 6061 alloy.

The ultimate and yield strengths of the as-received 1100 alloy were determined to be 140 and 128 MPa (20.3 and 18.6 ksi), respectively. The corresponding val-

ues reported in the literature (Ref. 11) for the H14 condition are 124 and 117 MPa (18 and 17 ksi).

Pure silver (99.99%) was used as the intermediate layer between the aluminum and stainless steel parts. Cylindrical specimens, each 12.6 mm (0.5 in.) in diameter and 63.5 mm (2½ in.) long, were machined from aluminum and stainless steel stock. The surface to be coated with silver was then lapped with alumina powder to within 0.5–1.0 wavelength of monochromatic light (0.1 μm). Lapped surfaces were cleaned with trifluorotrichloroethane and introduced into a hot hollow cathode (HHC) system for subsequent coating operations.

Use of the HHC process to coat surfaces before welding them has been described in previous publications (Refs.

Table 1—Material Chemical Analysis

Material	Element	Weight percent (wt-%)
Aluminum 99.99 percent pure ^(a) Annealed condition	Ca	0.00001
	Cu	0.00007
	Fe	0.0003
	Pb	0.00003
	Mg	0.00001
	Mn	0.00001
	Si	0.0002
	Al	Bal
Aluminum 6061 ^{(b),(c)} American Metal Society (AMS) 4150 Condition T6 (At start of evaluation)	Cr	0.2 (0.04–0.35)
	Si	~0.6 (0.4–0.8)
	Fe	0.2 (0.7 max)
	Cu	0.2 (0.15–0.40)
	Mn	0.07 (0.15 max)
	Mg	0.9 (0.8–1.2)
	Zn	0.02 (0.25 max)
	Ti	0.01 (0.15 max)
	Ga	0.01
	Zr	trace
	Al	97.8
Aluminum 1100 ^{(b),(c)} Condition H14 American Society for Testing and Metals (ASTM) B-221	Si	~0.8 (1.0 max)
	Fe	0.5 (0.05–0.20)
	Cu	0.1
	Mn	≤0.004 (0.05 max)
	Mg	≤0.5
	Cr	≤0.001
	Zn	0.02
	Ti	0.01
	Ni	0.1
	Misc. (Ga, Zr)	<0.008
	Al	98.3 ⁺ (99 ⁺)
Stainless Steel 316 ^(d) per QQ-S-763D condition A	C	0.053
	Mn	1.54
	P	0.026
	S	0.024
	Si	0.58
	Cr	17.19
	Ni	10.94
	Mo	2.17
	Cu	0.45
	Co	0.15
	N	0.036
	Fe	Bal

(a) Cominco American Electronics Materials Division, Spokane, WA 99216.

(b) Analysis conducted as part of the study.

(c) Quantities in parentheses are typical values as reported in *Aluminum Standards and Data* (Ref. 11).

(d) Joseph T. Ryerson and Son, Inc., Chicago, IL 60680.

*1 μm = 0.00004 in.

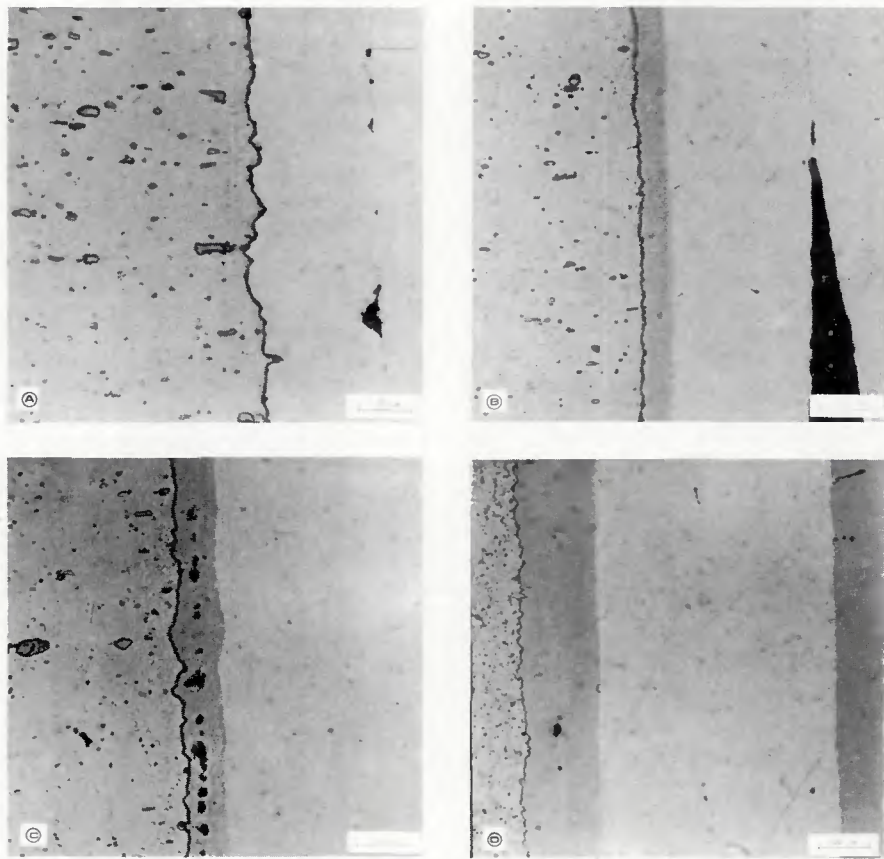


Fig. 1—Weld interface between stainless steel and 1100 aluminum alloy: A—unaged condition; B—after aging at 513 K for 4 h; C—after aging at 513 K for 16 h; D—after aging at 513 K for 49 h

10, 12-14). In this work, for any given material, 24 specimens were placed on a rotating substrate holder and were first ion-etched through the application of a bias voltage of 2 kV in a plasma of argon. Typically under these conditions, a layer of 750 Å* thick is sputtered off the stainless steel and corresponding layers of 11750, 4250, and 6250 Å thick are removed from the pure, 6061, and 1100 aluminum samples. Following this step, the bias voltage is removed and the electron beam power is increased to raise the evaporation rate of the silver. A silver coating of 25 µm thickness is deposited on each surface.

Stainless steel specimens coated in this fashion were welded to coated aluminum alloys at 477 K (399°F) for 10 min under an axial pressure of 103 MPa (149 ksi) following procedures described before (Refs. 5, 9, 10). Welding was achieved in air in a hydraulic press in which the specimens were heated by induction to the desired temperature of 477 K (399°F). Following welding, the specimens were machined into tensile testing configurations with a 7.6 mm (0.3 in.) diameter for the test region contain-

ing the solid state weld between the steel and the aluminum alloys.

The next step involved the aging of the specimens at the selected temperatures of 423, 473, and 513 K (302, 392, and 464°F). Aging was done for periods of time ranging from zero to 225 h and involved three samples for each condition for the three types of welds investigated (stainless steel/pure aluminum, stainless steel/1100 aluminum alloy, and stainless steel/6061 aluminum alloy). A Delta Design, Inc., cabinet furnace was typically preheated for one hour at the desired temperature before the introduction of the samples. Because of the relatively small size of the specimens, thermal equilibration was attained within a relatively short period of time, typically 5 min. The set furnace temperature was controlled to within a maximum deviation of 3 K (4.7°F) throughout all aging experiments.

Tensile testing of the aged specimens was made on a Baldwin tensile testing machine (model PTF-105). Prior to testing, the samples were cooled in liquid nitrogen for 10-15 min and were maintained at this temperature during testing. This was necessary to ensure that failure during tensile testing occurs in the welded joint rather than in the bulk aluminum.

All specimens were tested at a strain rate of 1.0 mm/mm min in the silver welded joint. For metallographic observations, the specimens were cut perpendicular to the plane of the joint and then prepared using standard techniques employing MgO (0.05 µm) powder as a polishing medium. With a Zeiss (model Ultraphot II) metallograph, the resolution of the intermetallic thickness was $\pm 0.50 \mu\text{m}$. Identification of the intermetallic zeta and mu phases (Ag_2Al and Ag_3Al) was made quantitatively by a JEOL electron microprobe (model 733).

Results

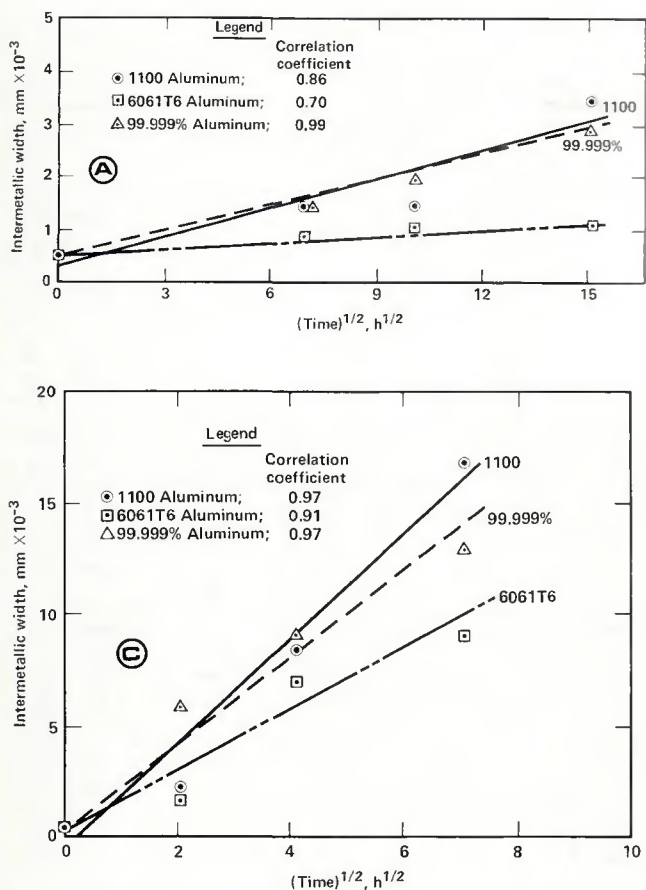
Microscopic observations of the as-bonded specimens showed little evidence for the existence of any intermetallic phase. In view of the earlier evidence by Doyle *et al.* (Ref. 9) that some (0.5 µm) Ag_2Al forms during welding, our observation may be limited by the resolution of the analytical method; this was as stated earlier, $\pm 0.5 \mu\text{m}$. Nevertheless, the results show clearly that an intermetallic phase develops and grows when the welded samples are subsequently aged.

Figure 1 shows a sequence of micrographs for the stainless steel/1100 aluminum alloy welds representing conditions of unaged (Fig. 1A) and aged for 4, 16, and 49 h, respectively, at 513 K (464°F). Similar observations were made on welds between the stainless steel and 6061 aluminum alloy and pure aluminum.

Quantitative results of the dependence of the intermetallic layer thickness on time for the three types of welds investigated are plotted in Fig. 2 for the aging temperatures of 423, 473, and 513 K (302, 410, and 464°F), respectively. In all cases, a linear dependence of thickness on the square-root of time is observed. With the exception of the 423 K (302°F) data, the statistical factors showing how well the curve fits the data (correlation coefficients) for the linear fit exceed 90%. In general, as can be seen from Fig. 2, the rate of growth of the intermetallic layer for joints with pure aluminum and with 1100 aluminum alloy are roughly the same. In contrast, the growth rate is significantly lower for joints between stainless steel and the 6061 alloy.

The effect of aging on the tensile strength of the welded specimens is shown in Fig. 3 for the three types of joints aged at 423, 473, and 513 K (302, 410, and 464°F), respectively. In these graphs the tensile strength is plotted vs. the square-root of the aging time. This is done to emphasize the influence of the intermetallic layer thickness on the decrease in joint strength. In this regard, the data for the 1100 alloy had the best fit to a linear behavior with correlation coef-

*1 Å = $3.9 \times 10^{-7} \text{ in.}$



ficients exceeding 90% for all temperatures.

A reasonable fit is also observed with the pure aluminum results, but considerable scatter was seen with the 6061 alloy data, especially the results obtained from the 513 K (464°F) aging experiments. In all cases, however, these results indicate essentially no change in the joint tensile strength when the aging is carried out at the lowest temperature, *i.e.*, 423 K (302°F). The apparent slight increase in the strength of the 1100 alloy welds is within the uncertainty of the results. It should be emphasized here that the tensile strengths of all three joints were determined at liquid nitrogen temperature.

Observations were also made on the mode of failure of the three types of joints investigated. This was done first by a semi-quantitative determination of the degree of adherence of the silver to the aluminum or stainless steel surfaces. Thus, the absence of silver regions on the failed surfaces would indicate a 100% adhesion failure. In contrast, if the fracture surface is completely covered with silver, it is designated as zero percent adhesion failure (*i.e.*, 100% cohesive failure).

The results showed that, with one exception, all 6061 alloy specimens failed in the silver layer, *i.e.*, with zero percent

adhesion failure. In contrast, the 1100 alloy specimens showed as high as 100% adhesion failure but had a typical average of 60%. The pure aluminum specimens had failures with as high as 62% adhesion failure and a typical average of 30%. There was no apparent trend of the percent adhesion failure with time or temperature for these materials.

Electron microprobe analyses were made on unaged specimens of all three types and on specimens which were subjected to the most severe aging conditions, *i.e.*, aged at the highest temperature for the longest time. In addition, one of two specimens showing a relatively high void concentration at the silver-silver interface was also analyzed. This particular specimen represents a stainless steel/6061 aluminum alloy weld which had been aged at 513 K (464°F) for 16 h and which had anomalously low tensile strength—see Fig. 3C. Analyses were made for Al, Ag, Mg, Si, and Fe for all specimens, and only a limited number of specimens were analyzed for S and Si. No systematic examinations were made for the minor alloying elements of Cu, Mn, Cr, Ti, and Zn, since they existed at such low levels they could not be detected.

Figure 4 shows a typical concentration distribution for Al at the aluminum alloy-silver interface for an unaged stainless

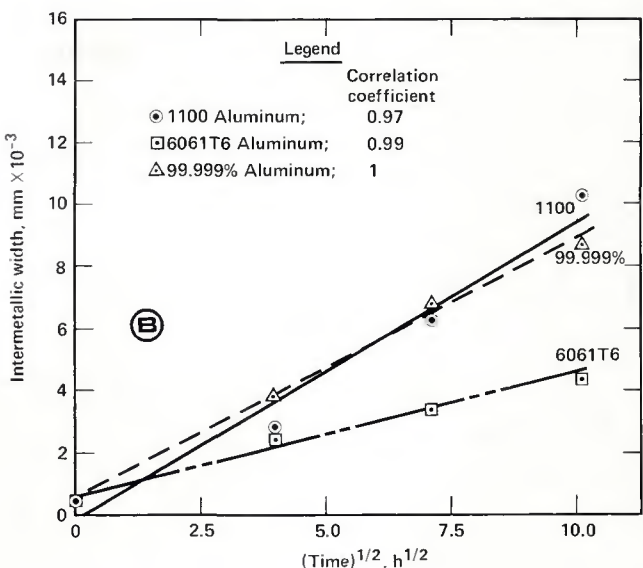


Fig. 2—The time dependence of the growth of the intermetallic layer:
A—T = 423 K; B—T = 473 K; C—T = 513 K

steel/6061 aluminum alloy sample. The lower (light) portion of this graph represents the 6061 alloy and the upper (dark) portion represents the silver region. No contrast is discernible for the silver-stainless steel interface. Figure 4 is typical of all unaged specimens for the three welds investigated.

Evidence for the formation of an intermetallic phase between silver and aluminum is clearly shown in the X-ray maps of Fig. 5. Figure 5 shows the development of the intermetallic layer after a 49 h aging at 513 K (464°F) for the Al/Ag interfaces for pure aluminum, 6061 aluminum alloy, and 1100 aluminum alloy, respectively. A similar analysis was done for the silver distribution in these samples. Generally, the resulting distribution maps are unrevealing except as indicators of the presence of voids, as shown in Fig. 6.

In Fig. 6, a line of voids at the original welding (Ag-Ag) interface is clearly seen; also shown are the interfaces between the 6061 and Ag (lower interface) and the stainless steel and Ag (upper interface) for a joint which was aged at 513 K (464°F) for 49 h. Concentration maps of this type gave little information concerning the distribution of the elements Mg, Si, and S. With respect to the distribution of Fe, the results show that iron atoms did not diffuse into the silver layer.

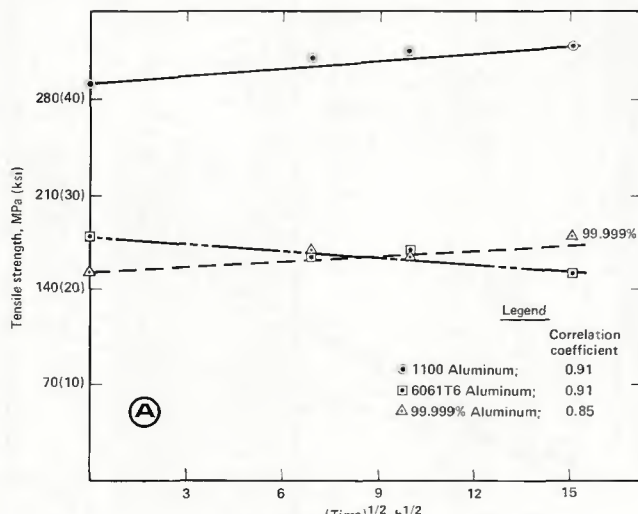
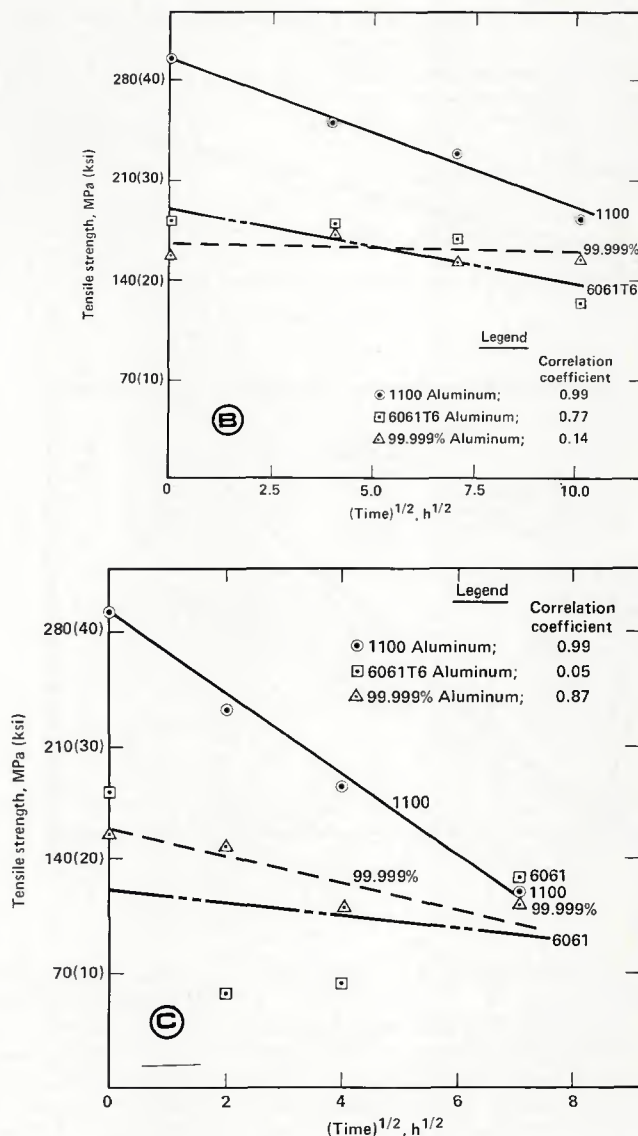


Fig. 3—The dependence of the weld strength on aging time: A— $T = 423\text{ K}$; B— $T = 473\text{ K}$; C— $T = 513\text{ K}$

Results of the quantitative distribution of silver and aluminum and other alloying elements are shown in Fig. 7 for the unaged 6061/stainless steel specimen. In Fig. 7A, the results are plotted in a linear form of weight-percent (wt-%) vs. distance (μm). The levels of Si and Mg are so low that they cannot be adequately discerned without plotting the results in a logarithmic form, as shown in Fig. 7B. Both levels, which are at approximately 1% in the aluminum phase, decrease drastically (by about two orders of magnitude) as one traverses the samples across the aluminum alloy-silver weld interface.

The distributions of Al and Ag at the Al/Ag interfaces for the three aged bonds are shown in Fig. 8 for the pure aluminum, 6061 alloy, and 1100 alloy,



respectively. For the case of the 6061 alloy, the distributions of Mg and Si were also measured and are shown in Fig. 9, which is a logarithmic plotting of the distribution shown in Fig. 8B.

Discussion

The degradation of the mechanical properties of joints between stainless steel and aluminum alloys as a result of the formation and growth of silver-aluminum intermetallic layers has been previously reported for 1100 aluminum alloy. No previous work has been conducted on stainless steel joints with 6061 aluminum alloy or with pure aluminum.

Figure 10 compares the results of this study on the 1100 alloy with the corresponding values reported by Naimon *et al.* (Ref. 10). The results of this study, as well as those referred to above, show an inverse linear dependence of the strength of the bond with the intermetal-

lic layer thickness. In the current study the results obtained from specimens aged at 423 K (302°F) showed little growth of the intermetallic with time and thus were not included in Fig. 10. The corresponding results for joints made with the 6061 alloy and with pure aluminum show considerable scatter—Fig. 11. However, an overall decrease of the strength with increasing intermetallic layer thickness is clearly evident.

As shown in Fig. 2A, the growth of the intermetallic layer for the 6061 alloy specimens was consistently lower than the other two types of aluminum materials. Intermetallic growth for pure aluminum specimens is reasonably close to that for the 1100 samples, especially at 423 and 473 K (302 and 410°F). The difference between the growth pattern of the intermetallic layer for the 6061 alloy and the other two aluminum materials cannot be attributed to the direct role of alloying elements in the growth process of this

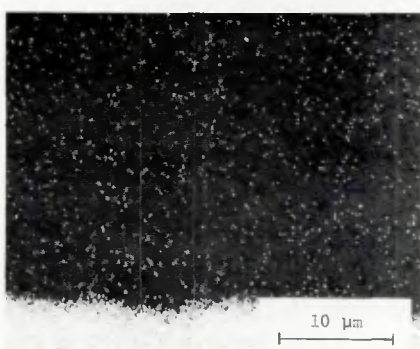


Fig. 4—Concentration distribution of Al at an unaged weld between stainless steel and 6061 aluminum alloy

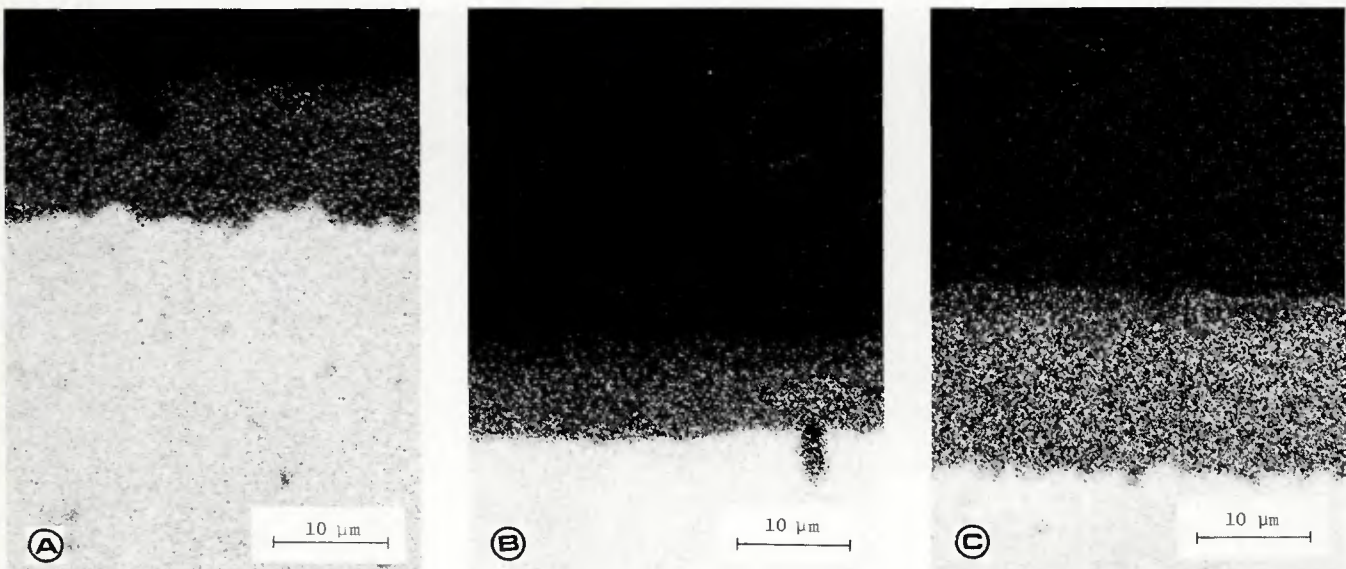


Fig. 5—X-ray maps showing aluminum distribution in welds with stainless steel after aging at 513 K for 49 h. Welds made as follows: A—With pure aluminum; B—with 6061 aluminum alloy; C—with 1100 aluminum alloy

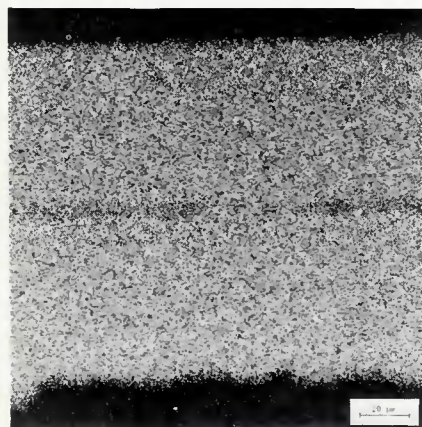


Fig. 6—Silver distribution at a stainless steel/6061 aluminum alloy weld aged at 513 K for 4 h. Dark line in the middle of this x-ray map is the consequence of voids

layer. The concentration levels of alloying elements in 6061 and 1100 alloys are comparable and are significantly higher than those for the "pure" aluminum specimens. However, as can be seen from the microprobe results (Fig. 9), Mg and Si diffuse from the 6061 alloy into the zeta-phase (Ag_2Al).

No similar behavior of these alloying elements could be detected in the 1100 alloy. The diffusion of Si and Mg took place during the aging process, as can be seen by comparing Figs. 9 and 7B. It is worth noting that these elements exist as a silicide phase, Mg_2Si , in the 6061 alloy.

As stated earlier, the growth of the total intermetallic layer is least in the case of the 6061 alloy. Since the thickness of the μ -phase (Ag_3Al) is approximately the same in all of these aluminum materials, it is possible to suggest that the existence of Mg and Si in the zeta-phase (Ag_2Al) may

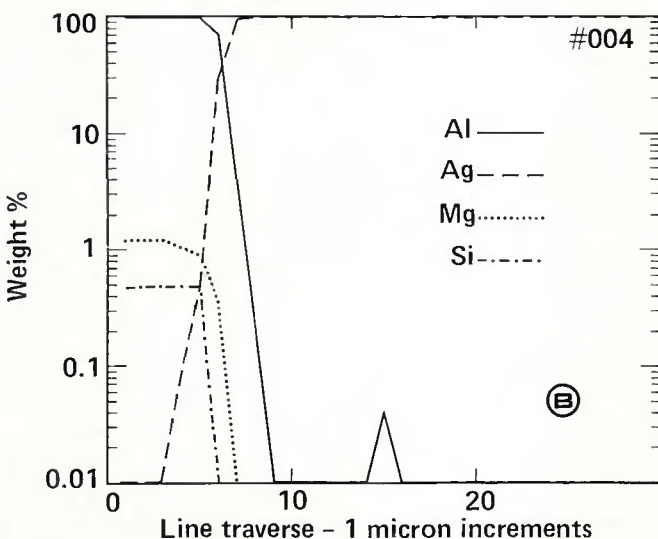
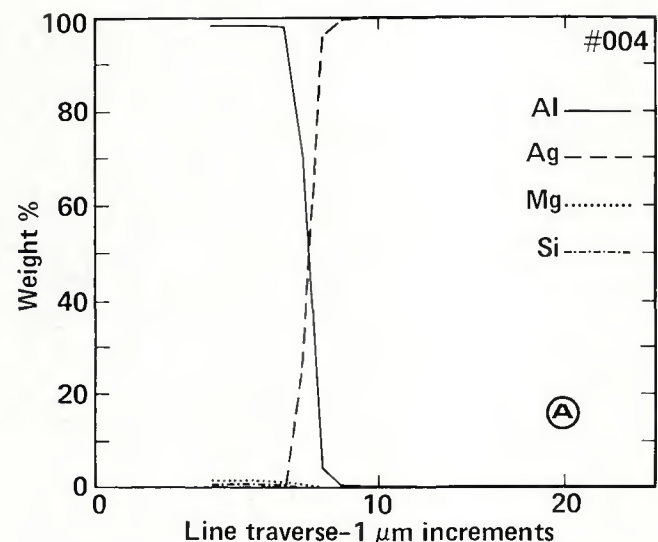


Fig. 7—Linear concentration profiles at a silver/6061 aluminum alloy weld interface; as-welded condition. A—linear concentration profile; B—logarithmic concentration profile

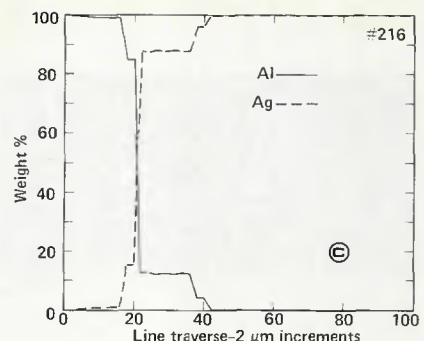
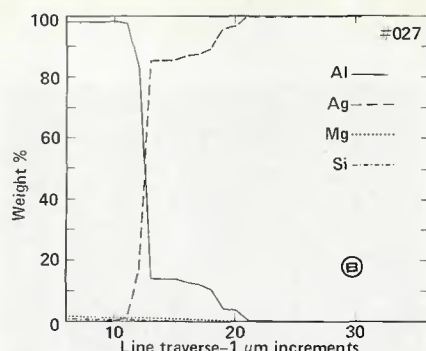
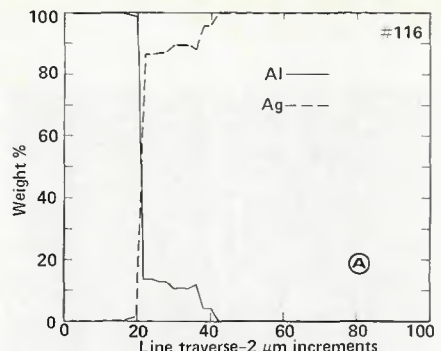


Fig. 8—Linear concentration profiles at a silver/aluminum or aluminum alloy weld interface. Specimens aged at 513 K for 49 h: A—pure aluminum; B—6061 aluminum alloy; C—6061 aluminum alloy

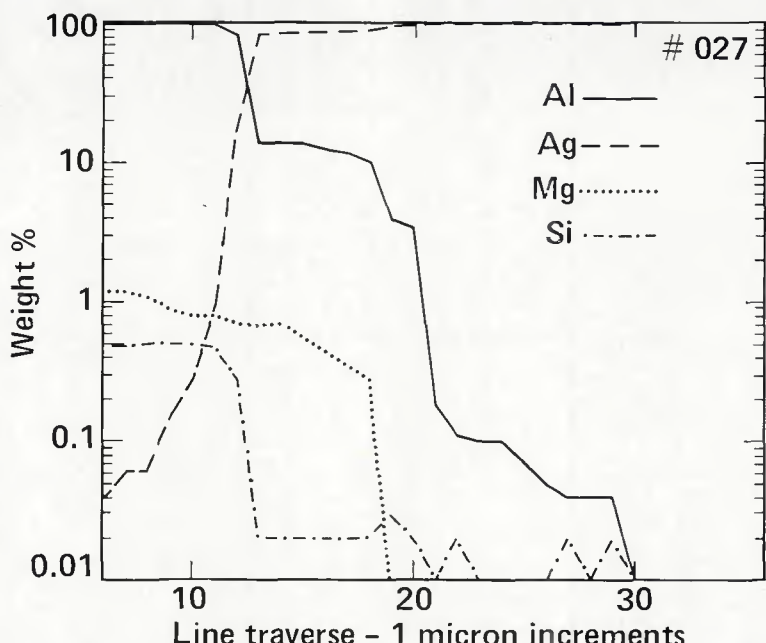


Fig. 9—Logarithmic concentration profiles at a silver/6061 aluminum alloy weld interface; specimen aged at 513 K for 49 h

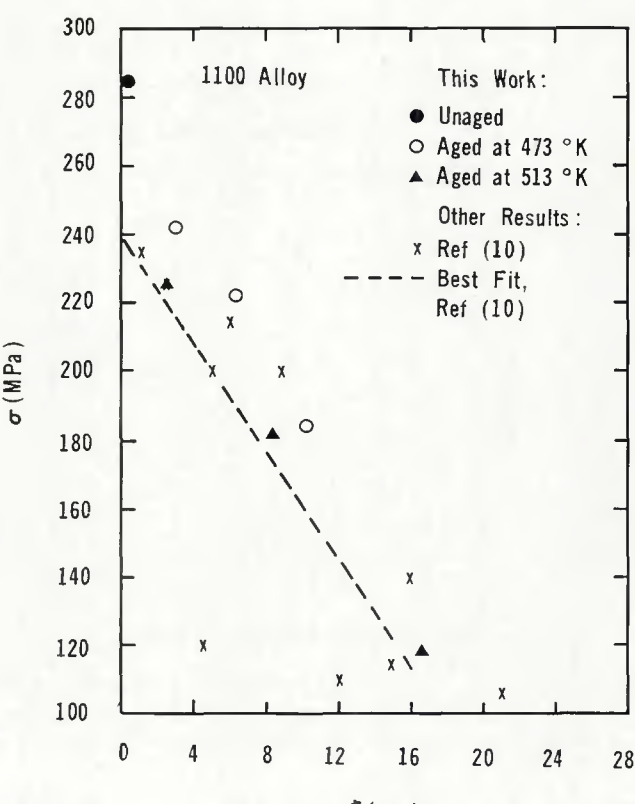


Fig. 10—The dependence of the strength of the weld between stainless steel and 1100 aluminum alloy on the total thickness of the intermetallic layer

hinder the growth of this phase. In general, the growth rate of the intermetallic layer was linear with the square-root of time. Such a dependence suggests a parabolic rate of growth which is controlled by diffusion in the intermetallic layer.

For the 1100 alloy, degradation of the mechanical properties of the joined specimens correlates very well with the increase in thickness of the intermetallic layer. However, a strong correlation is not obtained for the case of samples made with the 6061 alloy. The expectation of an influence by the intermetallic layer is based on the assumed failure of the joints at these layers because of their brittle nature. Obviously, this expectation is not justifiable, if the joint contains defects which play a more dominant role in the failure mode of the joint.

To evaluate such possibilities for the three materials investigated, fractographic examinations of selected samples were made. Unaged (as-welded) samples of all three types of materials failed cohesively, i.e., at the silver-silver interface. These fracture surfaces showed clear evidence of uncontacted (unwelded) regions. The 6061 alloy showed a higher percentage of uncontacted area relative to the other two materials—compare Figs. 12A and 12B.

Examples of contacted regions are outlined in black and are marked "a" in Fig. 12. For aged samples, the mode of failure of the 6061 alloy remained qualitatively the same, i.e., cohesive failure in the silver layer. However, specimens made from pure aluminum and from the 1100 alloy failed through a combination of cohesive failure and brittle failure in the intermetallic layer—Fig. 13A.

Cleavage separation in the fracture surface seen in Figs. 12 and 13 is evidence for the brittle nature of this failure. Under severe aging conditions for both of these materials, the failure was dominated by the brittle nature of the intermetallic layer. With milder aging, however, the pure aluminum samples tended to show more cohesive failure in contrast to the 1100 samples—Fig. 14A. X-ray dispersive analysis on fracture surfaces confirmed the presence of the intermetallic Ag_2Al in the severely aged 1100 and pure aluminum specimens and only Ag in the corre-

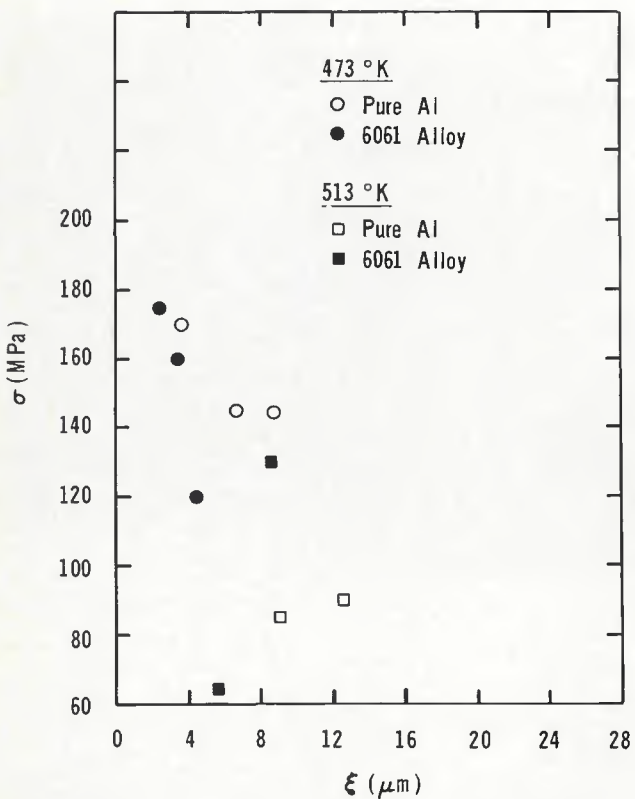


Fig. 11—The dependence of the strength of welds between stainless steel and pure aluminum and 6061 aluminum alloy on the thickness of the intermetallic layer

sponding 6061 specimens.

It is significant to note that metallographic observations of sections made normal to the original faying surfaces showed a significantly higher concentration of voids at the silver-silver (*i.e.*, faying) interface for the 6061 alloy than the other two specimens. Thus, the lack of a more exact correlation between the strength of the joint in this material and the thickness of the intermetallic layer is

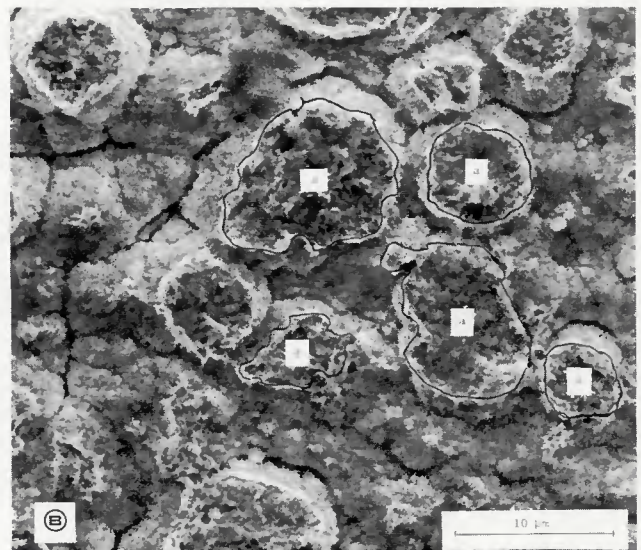
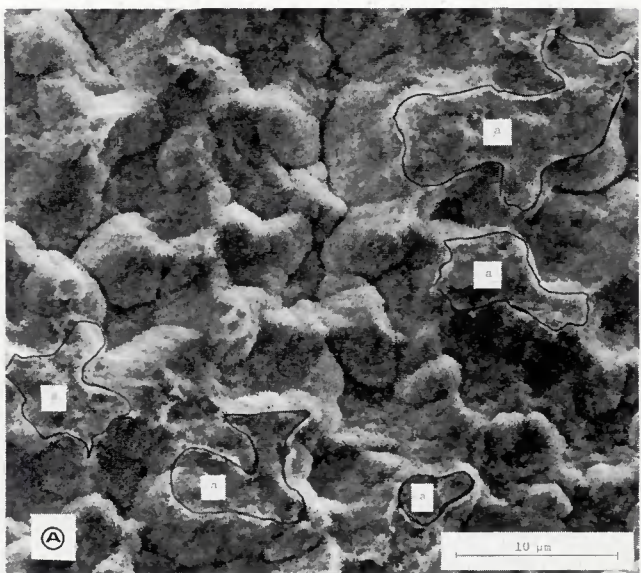


Fig. 12—Fracture surfaces of unaged welds: A—between stainless steel and pure aluminum; B—between stainless steel and 6061 aluminum alloy

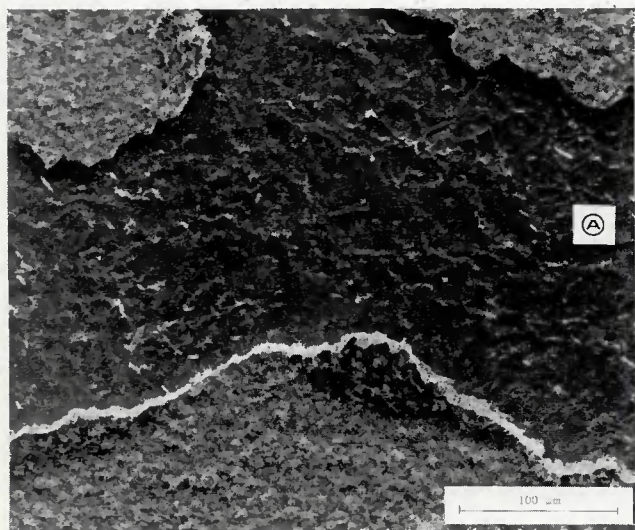
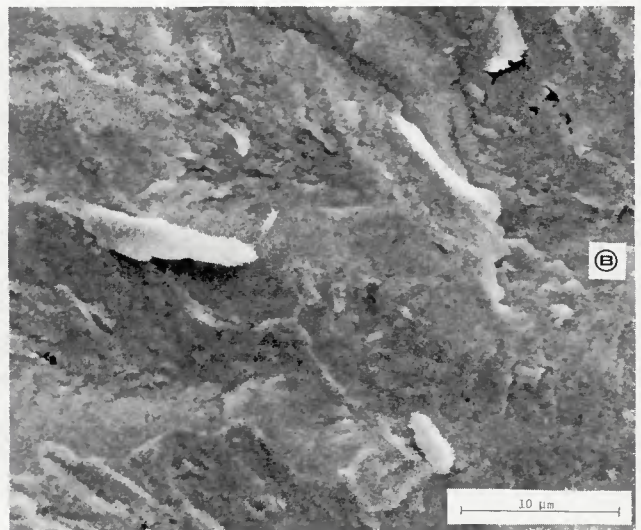


Fig. 13—Fracture surfaces of aged welds; specimens aged at 513 K for 49 h: A—between stainless steel and pure aluminum; B—between stainless steel and 1100 aluminum alloy



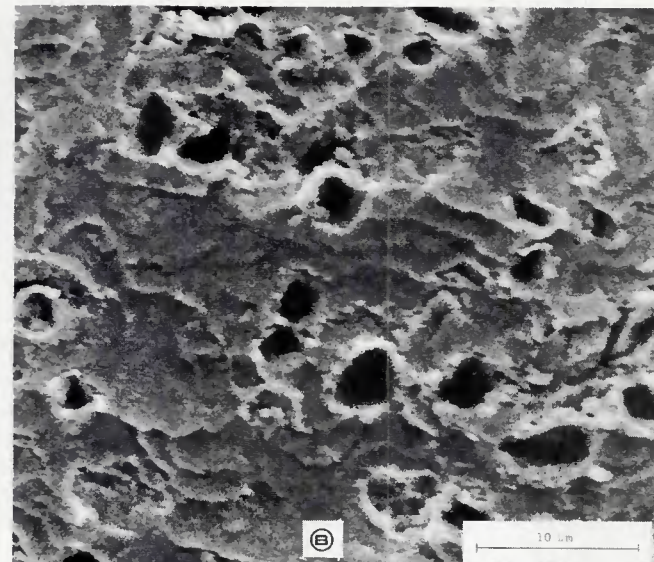


Fig. 14—Fracture surfaces of aged welds; specimens aged at 423 K for 225 h: A—between stainless steel and pure aluminum; B—between stainless steel and 1100 aluminum alloy

the result of the contribution of the voids to the failure process. The detrimental effect of voids on weld strength has been pointed out in a previous study (Ref. 12), and the low joint strength obtained for samples aged at 513 K (464°F) for 4 and 16 h (see Fig. 3C) is attributed to the existence of a high concentration of voids at the silver-silver interface.

Conclusions

1. The aging of diffusion welded specimens of Type 316 stainless steel with 99.999% pure aluminum, and 1100 and 6061 aluminum, resulted in the nucleation and growth of an intermetallic layer at the Al/Ag interface. The growth of this layer was found to have a generally linear dependence on the square-root of time at any given aging temperature. The rates of growth of the intermetallic layer for the pure aluminum and the 1100 aluminum alloy were similar, but were considerably higher than the corresponding value for the 6061 alloy. The observed segregation of Si and Mg at the intermetallic layer is proposed as a possible cause of the low rate of growth of the intermetallic layer in the case of the 6061 aluminum alloy.

2. Aging of the welded specimens resulted in a decrease in their tensile strength. The decrease in strength had a

generally direct correlation with the thickness of the intermetallic layer.

3. Welds between stainless steel and pure Al, the 1100 aluminum alloy, and the 6061 aluminum alloy failed in significantly different modes. Welds between stainless steel and the 6061 aluminum alloy failed almost exclusively in the cohesive mode, i.e., at the silver-silver interface. In contrast, welds made with the 1100 alloy failed in a predominantly adhesive mode, i.e., at the silver-aluminum or silver-stainless steel interfaces. Welds between stainless steel and pure aluminum failed in a combination of adhesive and cohesive modes.

4. Metallographic observations on sectioned joints of the three types of welds showed a consistently higher concentration of voids at the weld (i.e., silver-silver) interface for the case of the 6061 aluminum alloy. This is believed to provide an explanation for the relatively poor correlation between the thickness of the intermetallic layer and the tensile strength of welds made with this alloy.

References

1. Gerken, J. M., and Owczarski, W. A. 1965 (October). *A review of diffusion welding*. Welding Research Council bulletin 109.
2. King, W. H., and Owczarski, W. A. 1967. Diffusion welding of commercially pure titanium. *Welding Journal* 46(7):289-s to 298-s.
3. Barta, I. M. 1964. Low temperature diffusion bonding of aluminum alloys. *Welding Journal* 43(6):241-s to 247-s.
4. Crane, C. H., Lovell, D. Y., Baginski, W. A., and Olsen, M. G. 1967. Diffusion welding of dissimilar metals. *Welding Journal* 46(1):23-s to 31-s.
5. O'Brien, M., Rice, C. R., and Olsen, D. L. 1976. High strength diffusion welding of silver coated base metals. *Welding Journal* 55(1):25-27.
6. Hauser, D., Kammer, P. A., and Dedrick, J. H. Solid-state welding of aluminum. *Welding Journal* 46(1):11-s to 22-s.
7. Knowles, J. L. 1970. *High-strength, low-temperature bonding of beryllium and other metals*. Report UCRL-50766. Livermore, California: Lawrence Livermore Laboratory.
8. McEwan, K. J. S., and Milner, D. R. 1962. Pressure welding dissimilar metals. *British Welding Journal* 9(7):406-420.
9. Doyle, J. H., Capes, J. F., Johns, W. L., Rafalski, A. L., and Naimon, E. R. *Silver-aluminum intermetallic growth rates*. Report PMD-81-004. Golden, Colorado: Rockwell International, Rocky Flats.
10. Naimon, E. R., Doyle, J. H., Rice, C. R., Vigil, D., and Walmsley, D. R. 1981. Diffusion welding of aluminum to stainless steel. *Welding Journal* 60(11):17-20.
11. The Aluminum Association, Inc. 1979. *Aluminum standards and data*. Washington, D.C.
12. Williams, D. G. 1974. *Vacuum coating with a hollow cathode source*. *J. Vac. Sci. Technol.* 11:374.
13. Mah, G., McLeod, P. S., and Williams, D. G. 1974. Characterization of silver coatings deposited from a hollow cathode source. *J. Vac. Sci. Technol.* 11:663.